Skeletal Radiol (2014) 43:89–93
DOI 10.1007/s00256-013-1715-3

CASE REPORT

Intraosseous hemangioma arising in the clavicle

Yoshihiro Matsumoto · Yusuke Takahashi · Akihisa Haraguchi · Tatsuro Okamoto · Katsumi Harimaya · Tomoya Matsunobu · Makoto Endo · Yoshinao Oda · Yukihide Iwamoto

Received: 29 April 2013 / Revised: 6 August 2013 / Accepted: 8 August 2013 / Published online: 30 August 2013

Abstract Intraosseous hemangioma (IH) is commonly seen in the vertebral column and skull: however, IH occurring in the appendicular skeleton, including the clavicle, is uncommon. We herein report the case of a 69-year-old female presenting with IH of the left clavicle. The findings of preoperative imaging studies, including radiographs, computed tomography (CT), magnetic resonance imaging, fluorine-18-fludeoxyglucose (^{18}F-FDG) positron emission tomography (PET)/CT and ultrasonography, are described. In particular, ^{18}F-FDG PET/CT showed an ill-defined osteolytic lesion with abnormally high FDG uptake. Surgical en bloc resection with preoperative embolization was carried out and a histopathological examination confirmed the presence of an intraosseous cavernous hemangioma in the clavicle.

Keywords Intraosseous hemangioma · Clavicle · PET/CT

Introduction

Hemangiomas are benign, slow-growing, vascular tumors. Intraosseous hemangioma (IH) is most commonly seen in the vertebral column and skull [1]. In contrast, IH of the appendicular skeleton is uncommon [2]. The relative rarity of these lesions and the great variability of their radiological characteristics may suggest a more aggressive process, or possibly a malignant bone tumor [3]. We herein report the case of a 69-year-old female presenting with IH of the left clavicle. To our knowledge, this is the first English-language case report of a clavicle hemangioma that provides detailed radiological and histological findings along with a review of the literature.

Case report

A 69-year-old female presented with pain and swelling in the left clavicle region lasting for 1 year. The patient had no

Y. Matsumoto (✉) · A. Haraguchi · K. Harimaya · T. Matsunobu · M. Endo · Y. Iwamoto
Department of Orthopaedic Surgery, Graduate School of Medical Sciences, Kyushu University, 3-1-1 Maidashi, Higashi-ku, Fukuoka 812-8582, Japan
e-mail: ymatsu@ortho.med.kyushu-u.ac.jp

A. Haraguchi
e-mail: hachikou814@yahoo.co.jp

K. Harimaya
e-mail: harimaya@ortho.med.kyushu-u.ac.jp

T. Matsunobu
e-mail: matsunob@ortho.med.kyushu-u.ac.jp

M. Endo
e-mail: mako2endo@gmail.com

Y. Iwamoto
e-mail: yiwamoto@ortho.med.kyushu-u.ac.jp

Y. Takahashi · Y. Oda
Department of Anatomic Pathology, Graduate School of Medical Sciences, Kyushu University, 3-1-1 Maidashi, Higashi-ku, Fukuoka 812-8582, Japan

Y. Takahashi
e-mail: yuusuke@surgpath.med.kyushu-u.ac.jp

Y. Oda
e-mail: oda@surgpath.med.kyushu-u.ac.jp

T. Okamoto
Department of Surgery and Science, Graduate School of Medical Sciences, Kyushu University, 3-1-1 Maidashi, Higashi-ku, Fukuoka 812-8582, Japan
e-mail: tatsuro@surg2.me.kyushu-u.ac.jp

Fig. 1 Radiograph of the left clavicle showing a large, expansive and lobular lytic lesion with an ill-defined margin (*arrows*). Internal calcification was also observed

history of trauma or fracture of the left clavicle. A physical examination showed an ovoid mass measuring 6~7 cm in size in the left clavicle. A palpable pulsation of the mass was also observed. Laboratory values were within the normal ranges.

A radiograph revealed an expansive and osteolytic lesion and focally cortical thinning in the proximal part of the left clavicle (Fig. 1). A computed tomography (CT) scan clearly demonstrated a mass measuring 6 cm in size with an ill-defined margin. The mass was osteolytic and expansive and contained multiple calcified areas. Thinning and breaching of the cortex of the clavicle was also seen (Fig. 2). A magnetic resonance imaging (MRI) scan disclosed a mass in the medial side of the left clavicle. A lobular expansive mass was noted with heterogeneous hyperintensity on T2-weighted imaging with multiple curvilinear low signal intensities and punctate signal void. On T1-weighted imaging, the mass was heterogeneous iso and high-intensity to muscle with multiple punctate low signal as well as several foci of increased signal (Fig. 3). A gadolinium-enhanced T1-weighted imaging showed relatively heterogeneous enhancement and punctate non-enhancing low signal lesions were also observed (Fig. 3). On ^{18}F-FDG-positron emission tomography/CT (PET/CT), the lesion exhibited increased isotope uptake (SUV_{max}=4.7) (Fig. 4). Remarkably, ultrasonography showed a hypoechoic ovoid mass with multiple calcified areas and acoustic shadowing. Increased vascularity was also evident in the mass (Fig. 5). All of these imaging findings, in addition to the clinical presentation, indicated the vascular nature of the mass, particularly suggesting an IH. An open biopsy was performed, and a diagnosis of clavicle hemangioma was made.

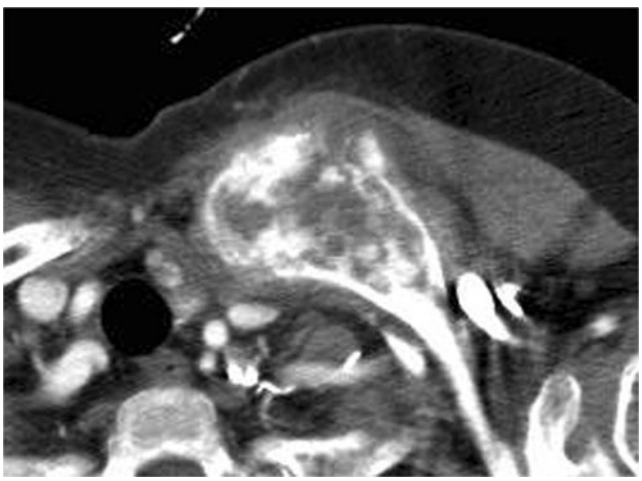

Fig. 2 Computed tomography image showing an osteolytic and expansive lesion with multiple calcified areas. Thinning and breaching of the cortex of the clavicle was also observed

Preoperative arterial embolization was carried out. The surgery consisted of extirpation of the tumor, and an anterolateral thoracotomy was performed in the left first intercostal space that proceeded to an upper median sternotomy. Then, the first rib and proximal portion of the sternum were resected and the feeding arteries of the tumor were ligated. The clavicle was cut at the distal region, and en bloc resection of the tumor was completed. The patient's post-operative course was uneventful. With respect to the gross appearance, a red-brownish and sponge-like mass encasing the clavicle was observed (Fig. 6). Microscopy showed proliferation of variable-sized, thin-walled vessels lined by endothelial cells (arrows in Fig. 7b) accompanied by hemorrhage and blood clots (asterisks in Fig. 7b). Reactive bone formation with focal dystrophic calcification (arrows in Fig. 7a), which might have been related to the calcified matrix seen on the CT scan and multiple punctate foci of the signal void seen on MRI, was also observed. Immunohistochemically, the endothelial and pericyte cells were positive for CD-31 (arrows in Fig. 7c) and CD-34 (arrows in Fig. 7d), and a definitive diagnosis of cavernous hemangioma of the clavicle was made. There was no evidence of malignancy.

Discussion

Based on the published surgical series, IH lesions account for approximately 1 % of all osseous tumors that were biopsied [1], with most cases occurring in the vertebral body or skull. Involvement of the appendicular skeleton has only rarely been

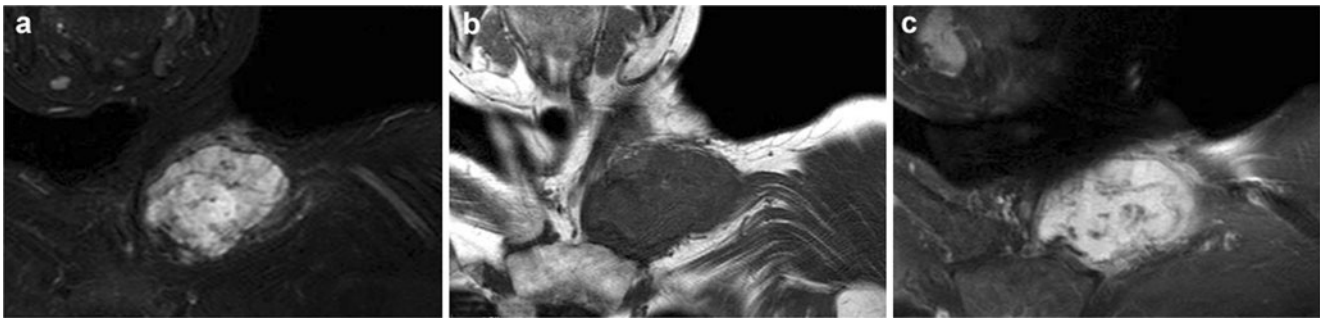

Fig. 3 Magnetic resonance imaging showing a lobular expansive mass with homogeneous hyperintensity on a T2-weighted image (**a**) and isointensity to muscle on a T1-weighted image (**b**). A gadolinium-enhanced T1-weighted image (**c**) shows homogeneous enhancement of the lesion. A punctuate signal void was observed in the internal area of the tumor

reported [4, 5]. In cases of spinal and skull IH, the lesions are typically found incidentally and symptoms are usually absent, as only 1 % of such patients have symptomatic lesions [6]. Unlike IH occurring in the spine and skull, most IH tumors involving the extra-axial skeleton cause clinical symptoms, such as local pain and swelling around the lesion [7] and the incidence of symptoms in such cases is considered to be high [3]. Histologically, hemangiomas can be classified as cavernous, capillary, venous, or mixed depending on the type of vascular involvement [7]. Cavernous hemangioma is the most common type observed in the peripheral bones, accounting for half of reported cases [7]. Capillary hemangioma is also observed in 10 % of all types, as reported in the literature [8]. Hemangiomas are slow

Fig. 4 Fluorine-18-fludeoxyglucose (^{18}F-FDG) positron emission tomography (PET)/CT image. **a** A lesion with high uptake (*arrow*) on the medial side of the left clavicle was observed on a coronal PET maximum intensity projection. **b** The lesion demonstrated abnormally high FDG uptake (SUV_{max}=4.7) on an integrated ^{18}F-FDG PET/CT image

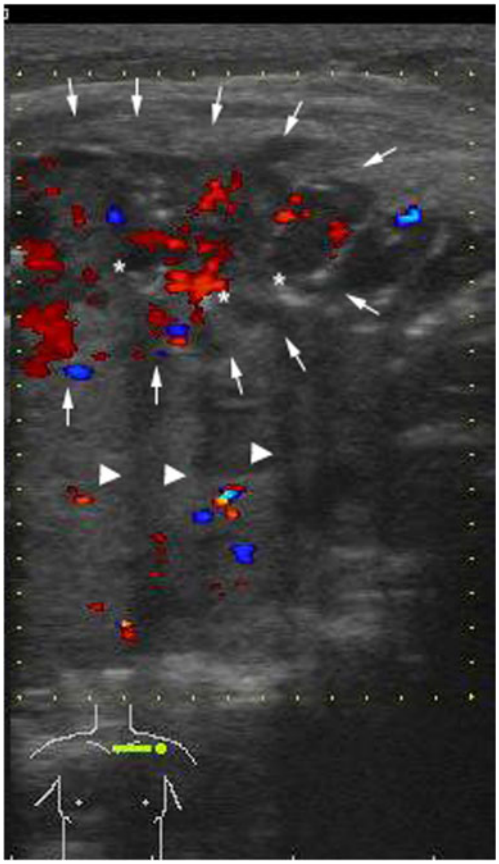

Fig. 5 Ultrasonography image showing a hypoechoic ovoid mass (*arrows*) with a large, high-flow vessel in the mass. The tumor contained multiple calcified areas (*asterisks*) and acoustic shadowing (*arrowheads*)

growing, and their capacity for malignant degeneration is generally unknown.

IH occurring in the long or flat bones presents a challenge in terms of the differential diagnosis of primary bone tumors, since the lesions are very rare and the radiographic findings

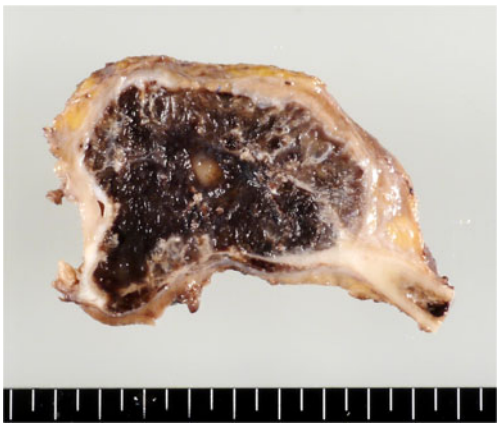

Fig. 6 Macroscopic appearance of the resected tumor. The specimen revealed a red-brownish and sponge-like mass encasing the clavicle

are variable and nonspecific. Clinically, these lesions have predilection for the metaphyseal/diaphyseal region, predominantly in the lower extremity in middle-aged females (4th and 5th decades of life) [3, 7]. Radiographically, IH may demonstrate the following characteristic features: (1) multi-lobulated lucent areas with surrounding fine trabecular bone, producing a honeycomb or soap bubble-like appearance, (2) well-circumscribed and punched-out radiolucent area, which may resemble multiple myeloma or metastatic bone tumors, (3) large and purely osteolytic cyst-like lesions with sclerotic margins, that mimic giant cell tumors of the bone, aneurysmal bone cyst, and fibrous dysplasia [3, 7, 9]. CT allows for the evaluation of the extent of the tumor and its relationship to surrounding structures. CT also clearly demonstrates the lobular architecture of osteolytic lesions as well as coarse trabeculation and matrix mineralization [3]. The MRI findings of IH vary according to the proportion of vascular and lipomatous soft tissue elements [10]. In this case, few lipomatous elements were observed in the tumor, and the tumor was composed primarily of vascular structures, as confirmed in the surgical specimen. Such lesions exhibit relatively homogeneous iso to low signal intensity on T1-weighted imaging and high signal intensity on T2-weighted imaging, probably owing to a slow blood flow [11]. The results of ultrasonography, that is, heterogeneous echogenicity, hypervascularity, and multiple calcified areas with acoustic shadowing, are similar to those seen for soft tissue hemangioma in the extremities [12]. Therefore, these features may also support the diagnosis of IH.

In some cases, intramedullary IH may show an aggressive expansive pattern that mimics malignant bone tumors, including angiosarcomas. Previous studies have described PET/CT imaging as an accurate method for the pre-operative staging of bone and soft tissue sarcomas [13]. However, the clinical use of PET/CT to differentiate between malignant and benign musculoskeletal tumors is controversial because high FDG uptake has been detected in some benign tumors, including schwannomas, giant cell tumors, and chondroblastomas [13]. Hemangiomas are considered to be a metabolically stable benign tumors on PET/CT [14], and the SUV_{max} for FDG in 16 hemangiomas, including soft tissue and osseous tumors, has been reported to range from 0.73 to 1.67 [14]. In contrast, in this case, the SUV_{max} was 4.7 on a PET/CT scan, which is more than two times higher than the previously suggested cut-off point (SUV_{max}=2.0) [15]. Similar atypical high uptake was also reported in a case of IH of the tibia [6]. Therefore, the usefulness of PET/CT for differentiation of IH from malignant bone tumors should be further investigated.

In conclusion, IH involving the extra-axial skeleton can present a wide variety of radiologic features. It can present as an expansive, osteolytic lesion with increased 18F-FDG

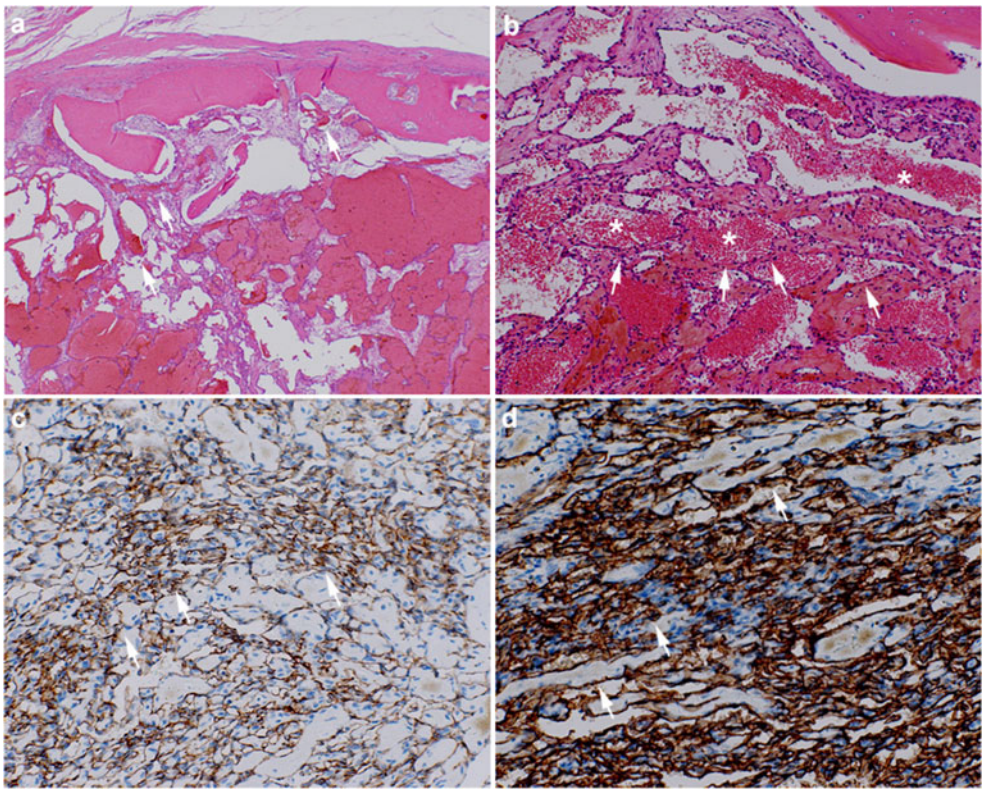

Fig. 7 Photographs of the pathological specimens. **a**, **b** Hematoxylin and eosin (H&E) staining of the resected specimen reveals the proliferation of variable-sized, thin-walled vessels lined by endothelial cells (*arrows* in **b**), accompanied by hemorrhage and blood clots (*asterisks* in **b**). Reactive bone formation with focal dystrophic calcification (*arrows* in **a**) (original magnification, ×40 in **a**, ×100 in **b**). **c**, **d** An immunohistochemical analysis of a cluster of differentiation (CD) 31 (*arrows* in **c**) and CD34 (*arrows* in **d**). The endothelial and pericyte cells in the tumor are positive for CD-31 and CD-34 (original magnification, ×200)

uptake on PET/CT mimicking a malignant bone tumor as shown in this case. The final diagnosis in this report was confirmed by histopathological examination; however, we observed the thrill of the tumor and characteristic ultrasonographic features, suggesting the tumor as IH of the clavicle.

Acknowledgments This work was supported by a Grant-in-Aid for Scientific Research from the Japan Society for the Promotion of Science (#23592192).

Conflict of Interest The authors have no conflicts of interest to declare.

References

1. Unni KK. Dahlin's bone tumors: general aspects and data on 11,087 cases. 5th ed. Philadelphia: Lippincott-Raven; 1996.
2. Wenger DE, Wold LE. Benign vascular lesions of bone: radiologic and pathologic features. Skeletal Radiol. 2000;29:63–74.
3. Rigopoulou A, Saifuddin A. Intraosseous hemangioma of the appendicular skeleton: imaging features of 15 cases, and a review of the literature. Skeletal Radiol. 2012;41:1525–36.
4. Clements RD, Turnage RB, Tyndal EC. Hemangioma of the rib: a rare diagnosis. Am Surgeon. 1998;64:1027–9.
5. Puig J, Garcia-Pena P, Enriquez G, Huguet P, Lucaya J. Intraosseous haemangioma of the ilium. Pediatr Radiol. 2006;36:54–6.
6. Cha JG, Yoo JH, Kim HK, Park JM, Paik SH, Park SJ. PET/CT and MRI of intra-osseous haemangioma of the tibia. Br J Radiol. 2012;85:e94–98.
7. Kaleem Z, Kyriakos M, Totty WG. Solitary skeletal hemangioma of the extremities. Skeletal Radiol. 2000;29:502–13.
8. Dorfman HD, Czerniak B. Vascular lesions. Bone tumors. St. Louis: Mosby; 1998.
9. Resnick D, Kyriakos M, Greenway GD. Tumors and tumorlike lesions of bone. Diagnosis of bone and joint disorders - 4th ed. W.B. Saunders; 2002: 3979–3978.
10. Murphey MD, Fairbairn KJ, Parman LM, Baxter KG, Parsa MB, Smith WS. From the archives of the AFIP. Musculoskeletal angiomatous lesions: radiologic-pathologic correlation. Radiographics. 1995;15:893–917.
11. Vilanova JC, Barceló J, Smirniotopoulos JG, et al. Hemangioma from head to toe: MR imaging with pathologic correlation. Radiographics. 2004;24:367–85.
12. Chiou HJ, Chou YH, Chiu SY, Wang HK, Chen WM, Chen TH, et al. Differentiation of benign and malignant superficial soft-tissue masses using grayscale and color Doppler ultrasonography. J Chin Med Assoc. 2009;72:307–15.
13. Shin DS, Shon OJ, Han DS, Choi JH, Chun KA, Cho IH. The clinical efficacy of ^{18}F-FDG-PET/CT in benign and malignant musculoskeletal tumors. Ann Nucl Med. 2008;22:603–9.
14. Hatayama K, Watanabe H, Ahmed AR, et al. Evaluation of hemangioma by positron emission tomography: role in a multimodality approach. J Comput Assist Tomogr. 2003;27:70–7.
15. Dehdashti F, Siegel BA, Griffeth LK, et al. Benign versus malignant intraosseous lesions: discrimination by means of PET with 2-[^{18}F]fluoro-2-deoxy-D-glucose. Radiology. 1996;200:243–7.